



Title	Concept model of atomic hydrogen dry developing process for photolithographic patterning
Author(s)	Takemori, Yuki; Gohdo, Masao; Koda, Yuta et al.
Citation	AIP Advances. 2020, 10, p. 105223
Version Type	VoR
URL	<a href="https://hdl.handle.net/11094/87651">https://hdl.handle.net/11094/87651</a>
rights	This article is licensed under a Creative Commons Attribution 4.0 International License.
Note	

*The University of Osaka Institutional Knowledge Archive : OUKA*

<https://ir.library.osaka-u.ac.jp/>

The University of Osaka

# Concept model of atomic hydrogen dry developing process for photolithographic patterning

Cite as: AIP Advances **10**, 105223 (2020); <https://doi.org/10.1063/5.0027509>

Submitted: 29 August 2020 • Accepted: 27 September 2020 • Published Online: 15 October 2020

 Yuki Takemori,  Masao Gohdo,  Yuta Koda, et al.



View Online



Export Citation



CrossMark

## ARTICLES YOU MAY BE INTERESTED IN

Isotropic plasma atomic layer etching of  $\text{Al}_2\text{O}_3$  using a fluorine containing plasma and  $\text{Al}(\text{CH}_3)_3$

Applied Physics Letters **117**, 162107 (2020); <https://doi.org/10.1063/5.0022531>

Role of plasma parameters on the characteristics properties of flexible transparent ITO films deposited by 3D facing and planar facing magnetron sources

AIP Advances **10**, 105231 (2020); <https://doi.org/10.1063/5.0017519>

Copper dry etching by sub-atmospheric-pressure pure hydrogen glow plasma

Applied Physics Letters **109**, 211603 (2016); <https://doi.org/10.1063/1.4967382>



# Concept model of atomic hydrogen dry developing process for photolithographic patterning

Cite as: AIP Advances 10, 105223 (2020); doi: 10.1063/5.0027509

Submitted: 29 August 2020 • Accepted: 27 September 2020 •

Published Online: 15 October 2020



Yuki Takemori,<sup>1</sup> Masao Gohdo,<sup>2,a)</sup> Yuta Koda,<sup>1</sup> and Hideo Horibe<sup>1</sup>

## AFFILIATIONS

<sup>1</sup>Department of Applied Chemistry and Bioengineering, Graduate School of Engineering, Osaka City University, 3-3-138 Sugimoto, Sugimoto-ku, Osaka-shi, Osaka 558-8585, Japan

<sup>2</sup>The Institute of Scientific and Industrial Research, Osaka University, 8-1 Mihogaoka, Ibaraki-shi, Osaka 567-0047, Japan

<sup>a)</sup>Author to whom correspondence should be addressed: Masao Gohdo, [mgohdo@sanken.osaka-u.ac.jp](mailto:mgohdo@sanken.osaka-u.ac.jp)

## ABSTRACT

Atomic hydrogen dry etching was used for microstructure fabrication. Photolithography was proposed and achieved by a dry development process using atomic hydrogen irradiation. The reaction system of poly(methyl methacrylate) mixed with molecular benzophenone was examined as a model system for a proof-of-concept study. Optical patterning was experimentally made on a thin layer of poly(methyl methacrylate) with benzophenone by UV light exposure with a photomask. The reaction system acted as a negative tone resist in the proposed process. Thus, a model system for a new atomic hydrogen dry development process was proposed and successfully demonstrated.

© 2020 Author(s). All article content, except where otherwise noted, is licensed under a Creative Commons Attribution (CC BY) license (<http://creativecommons.org/licenses/by/4.0/>). <https://doi.org/10.1063/5.0027509>

## INTRODUCTION

Atomic hydrogen can be used to etch polymers,<sup>1–6</sup> silicon,<sup>7,8</sup> silicon-carbide,<sup>9</sup> and copper<sup>10</sup> without causing any oxidation. It is also known that atomic hydrogen can be used to carry out isotropic etching. The development of a photolithography technique using an atomic hydrogen dry development process will expand the range of potential applications of atomic hydrogen. Currently, two methods are used for the generation of atomic hydrogen; these methods were developed in the 1910s–1920s<sup>11,12</sup> and are now well understood.<sup>13,14</sup> The first method is based on the use of plasma chemical vapor deposition that is often used for diamond synthesis,<sup>15,16</sup> and the second method is catalytic chemical vapor deposition (Cat-CVD) using metal catalysts such as tungsten.<sup>11,13,17,18</sup> An etching process using hydrogen gas would be simpler and would have lower economic and environmental costs than the currently used etching processes. While it is difficult to obtain a realistic estimate of the costs of different industrial processes, it is clear that atomic hydrogen dry etching has the potential to use less solvent compared to the wet development processes and will use less toxic or halogenated gases compared to the other dry development processes.

The potential benefits of atomic hydrogen etching are based on the small size of the hydrogen molecule that is much smaller than the developer molecules used in wet development processes, enabling atomic hydrogen to penetrate into fine patterns. This feature is potentially beneficial for the miniaturization of the lithography process, even though the critical size of etching is restricted by the size of the volatile decomposed molecule. Another characteristic of atomic hydrogen is its electrical neutrality and reactivity. The neutrality of atomic hydrogen may give rise to difficulties in the anisotropic etching process because the application of an electric bias will not affect the trajectory of atomic hydrogen. The reactivity of atomic hydrogen is basically complementary to that of ozone etching. Polymers such as polystyrene, phenol resins such as the novolak resist, and poly(4-vinylphenol) show less reactivity with atomic hydrogen compared to poly(methyl methacrylate) (PMMA) but can be easily removed by the wet ozone treatment.<sup>1,4,19,20</sup> On the other hand, PMMA is easily removed by atomic hydrogen but is difficult to be removed by the wet ozone treatment. Thus, if these features were introduced to the easily etched polymer by photo-irradiation, and the irradiated area was converted to a hardly etched polymer, photolithography would be achieved. It is also expected that the optical conversion of a

laboriously etched polymer to an easily etched polymer will achieve the opposite tone resist.

In this work, photolithography using an atomic hydrogen dry development process on a thin layer of PMMA with benzophenone as a photo-reactive molecule was proposed and carried out experimentally for a proof-of-concept demonstration of this process. For this purpose, molecular benzophenone was used instead of the polymers that have a benzophenone moiety used in the UV-cross-linking adhesives<sup>21</sup> because the non-photoreacted area must be etched and must be volatile under reduced pressure. The same reaction system has been reported in the literature<sup>22</sup> and is used in this study to advance dry development using atomic hydrogen and for an experimental demonstration of photolithography.

## EXPERIMENTAL SECTION

### Sample preparation

PMMA (Aldrich,  $M_w = 120\,000$ ) was dissolved in ethyl lactate (Nacalai Tesque, 96.0%+), and a 12 wt. % solution was obtained. Both PMMA and ethyl lactate were used as received. A thin layer of this solution was used as a control material for atomic hydrogen dry etching. To obtain the BP/PMMA mixed solution, 9.0 wt. %, 19 wt. %, 41 wt. % of benzophenone (TCI, 99+%, BP) with respect to the weight of PMMA was dissolved in the PMMA/ethyl lactate solutions. BP was used after recrystallization from ethanol (Wako, 99+%). The solutions were spin-coated on a 3-in. silicon wafer using a spin coater (M-1S, Mikasa) and baked first at 60 °C for 1 min and then at 100 °C for 1 min to remove the solvent. The typical layer thickness was 1  $\mu\text{m}$ .

### Estimation of the selection ratio and patterning procedure

The initial layer thickness was determined using a stylus profiler (Dektak® 6M, Bruker). Then, lithographic exposure was carried out by irradiation with broad light exposure using a photomask with a mask aligner. A super-high-pressure UV discharge lamp (USH-250D with HB-25105AA power supply, Ushio) was used as the light source. The typical exposure intensity was measured by a thermal power sensor (S401C with PM100D, Thorlabs) as 55  $\text{mW}/\text{cm}^2$  for the broad illumination. The exposure dose estimation was performed at 365 nm using a photodiode-type detector (UVD-365PD with UIT-101, Ushio). Lithographic exposure was carried out at  $295 \pm 3$  K. To estimate the selection ratio under a certain exposure dose, light exposure was simply carried out without a photomask.

Atomic hydrogen was irradiated using the hot-wire method with a tungsten wire by an atomic hydrogen irradiator (Tokyo Ohka Kogyo Co, Ltd.), as schematically shown in Fig. 1. Hydrogen was introduced close to the tungsten wire with flow rate control ensured by a mass flow controller. The tungsten wire was heated by electrical heating with a constant current controlled by an AC power supply (max. voltage 200 VAC, 60 Hz). A sample was placed under the hot-wire on the sample stage with heating control in order to heat the sample. The heating stage and the area around the hot-wire were covered by a quartz plate and a quartz hood to reduce the loss of atomic hydrogen by avoiding the exposure of the metal surface

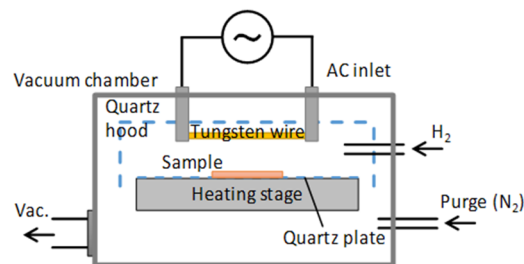


**FIG. 1.** Schematic diagram of the atomic hydrogen irradiator. The flow rate of the hydrogen gas was controlled to remain in the range of 90 ml/min–490 ml/min. Temperature control of the heating stage enables sample temperature control in the temperature range from room temperature to 200 °C.

to the generated atomic hydrogen with the exception of an uncovered area just below the hot-wire, so that the bare aluminum sample stage was exposed for an area that had a diameter of 77 mm and was well covered by a 3-in. wafer. A vacuum chamber was evacuated using a dry pump (EV-S50N, Ebara). A throttle valve was placed between the chamber and the pump to achieve the desired internal pressure by controlling the exhaust velocity. The temperature of the hot-wire was monitored through a quartz window using a two-color pyrometer (ISR 12-LO MB 33, Impac) placed outside the chamber.

The general procedure of atomic hydrogen irradiation was as follows. (1) The sample was placed on a temperature-equilibrated sample stage of an atomic hydrogen irradiator at a certain temperature. (2) The chamber was evacuated down to 3 Pa or less. (3) Hydrogen gas was introduced at a certain flow rate and a certain exhaust velocity setting, and atomic hydrogen was irradiated. (4) Thirty seconds after the hydrogen flow started, the power supply used to heat the hot-wire with a certain current setting was turned on, and atomic hydrogen irradiation was commenced once the hot-wire temperature increased. The temperature was stabilized at approximately 10 s after turning on the power supply. (5) These conditions were maintained until the atomic hydrogen irradiation was completed. (6) The power supply of the hot-wire was turned off, and the system was maintained for 30 s under hydrogen flow. (7) The hydrogen flow was stopped, and the chamber was evacuated to obtain a pressure of 3 Pa or less. (8) The vacuum chamber was purged with nitrogen gas up to atmospheric pressure, and then the sample was replaced or removed. In step 1 and after step 8, the sample was exposed to the atmosphere, while during steps 2–7, the chamber was evacuated using a dry pump. Under the atomic hydrogen irradiation conditions, the pressure was at a certain low vacuum value given by the flow rate of hydrogen gas and the setting of the throttle valve. Procedures 3–7 were automated to use the desired settings of the stage temperature, hydrogen flow rate, hot-wire current, throttle valve settings, and the duration of atomic hydrogen irradiation. In the present series of experiments, the stage temperature was maintained at 100 °C, the pressure during atomic hydrogen irradiation was 80 Pa, the hydrogen flow rate was 490 ml/min, and the temperature of the tungsten wire was 1800 °C.

After irradiation of the thin layer sample on the Si wafer for a certain time with atomic hydrogen, the thickness of the polymer

layer was determined using a stylus profiler. For the observation of the resultant pattern, optical microscopy images were obtained using an optical microscope (Eclipse L150, Nikon).

## RESULTS AND DISCUSSION

The thicknesses of the polymer layers were decreased by atomic hydrogen irradiation, and the magnitude of the thickness decrease was proportional to the irradiation duration. Therefore, the etching rates were calculated using linear fitting of the remaining layer thickness plotted as a function of the irradiation time. The etching rates obtained using different light exposure doses are listed in Table I. An examination of the data presented in Table I shows that the etching rates for the unexposed samples remained at approximately 0.1  $\mu\text{m}/\text{min}$ . When the BP/PMMA sample was exposed to a certain dose of light, the etching rates decreased with the increasing exposure dose. The selection ratio of this dry development process can be calculated by dividing the etching rate of the unexposed sample by that of the exposed sample. The obtained selection ratio shows a clear dose dependence for all BP/PMMA samples, as shown in Fig. 2. The maximum selection ratio was

TABLE I. Etching rate and selection ratio.

Sample	Light exposure		Atomic hydrogen dry etching	
	Dose <sup>a</sup> (J cm <sup>-2</sup> )		Etching rate ( $\mu\text{m min}^{-1}$ )	Selection ratio
0	...		0.094	...
	0		0.094	1.00
	2.2		0.066	1.42
	4.7		0.052	1.82
	8.7		0.046	2.04
	13.5		0.043	2.21
	20.3		0.040	2.37
	29.1		0.036	2.62
9.0	40.6		0.034	2.75
	0		0.099	1.00
	2.2		0.064	1.56
	4.7		0.049	2.03
	8.7		0.045	2.23
	13.5		0.041	2.44
	20.3		0.036	2.77
	29.1		0.035	2.88
19	40.6		0.032	3.12
	0		0.106	1.00
	2.2		0.062	1.72
	4.7		0.049	2.16
	8.7		0.043	2.46
	13.5		0.040	2.65
	20.3		0.037	2.88
	29.1		0.034	3.13
41	40.6		0.033	3.20

<sup>a</sup>Exposure doses are expressed as the value of the dose at 365 nm.

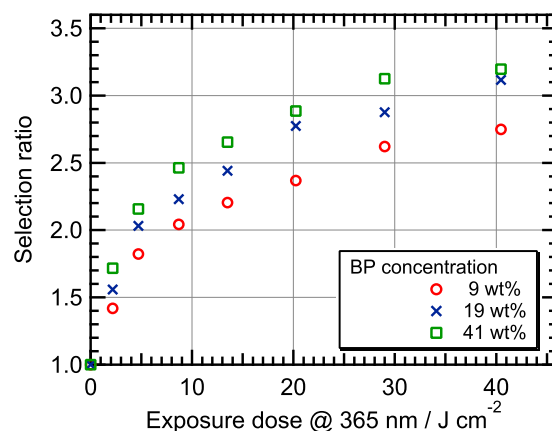


FIG. 2. Dependence of the selection ratio on the exposure dose and BP concentration.

achieved for the 41 wt. % BP-containing PMMA and was equal to 3.2. The selection ratio appeared to saturate close to the maximum dose in this series of experiments; however, when the selection ratio was plotted vs the exposure dose in a log-log plot, the dependence showed a clear linear relationship, as shown in Fig. S1. Based on this log-log plot, the selection ratio appears to have not yet been saturated.

The photoinduced reaction between BP and PMMA is well-known.<sup>23</sup> BP in the excited triplet state carries out a hydrogen abstraction reaction<sup>24</sup> with PMMA, resulting in a partial modification of PMMA.<sup>21,23,25–29</sup> Product analysis was also reported for this reaction, and it was found that the side reaction involves the formation of benzopinacol as determined by gel permeation chromatography. Due to the nature of hydrogen abstraction, the intermediate radical of BP is the benzophenone ketyl radical, which is a carbon-centered radical, and the hydrogen abstraction is irreversible. Three types of hydrogen atoms can react with the triplet carbonyl of BP, namely, the hydrogen atoms of the  $-\text{CH}_2-$  groups in the main chain, the hydrogen atoms of the  $-\text{CH}_3$  groups, and the hydrogen atoms of the  $-\text{O}-\text{CH}_3$  groups. The site of hydrogen abstraction will be mainly affected by the location of BP because the reaction occurred in solid PMMA around 23 °C, which is the temperature at which the light exposure was made, so that the diffusion of BP was limited. The counterpart radical of the hydrogen abstraction reaction in PMMA can lead to a cross-linking reaction. Based on the reported atomic hydrogen etching rates, polymers containing an aromatic ring tend to exhibit a low etching rate.<sup>1</sup> Therefore, it is reasonable to assume that the etching rate of the light-exposed area converted to a PMMA derivative, which is a random copolymer containing an aromatic ring, is also low.

As shown in Fig. 2, the selection ratio increased with the increasing exposure dose, and the observed selection ratio trend indicated that a lower BP concentration resulted in a smaller selection ratio. However, this trend was attributed to the fact that the etching rate of the unexposed area tends to be higher with the increasing BP concentration because BP will be simply sublimed and therefore undergoes higher etching, while the exposed area etching rates were comparable for all BP concentrations. Therefore, a



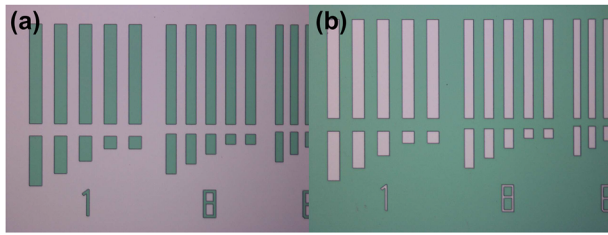


**FIG. 3.** Optical microscopy images of atomic hydrogen dry development photolithography. Broad light exposure of  $40.6 \text{ J/cm}^2$  at  $365 \text{ nm}$  with an etching duration of  $9 \text{ min}$  on the sample of  $19 \text{ wt. \% BP}$  vs  $\text{PMMA}$ . In the figure, 1, 8, and 6 correspond to  $100 \mu\text{m}$ ,  $80 \mu\text{m}$ , and  $60 \mu\text{m}$  line and space, respectively. Positive (a) and negative (b) line and space patterns.

higher concentration did not enhance the yield of BP grafting to PMMA, which can be understood based on benzopinacol formation.<sup>28,29</sup> Similar phenomena may occur when the exposure dose is increased. In addition to the benzopinacol formation, the steric issue mentioned above for hydrogen abstraction appears to limit the grafting yield because if BP could diffuse rapidly in PMMA within the lifetime of the excited state, a linear dose dependence would be observed until BP was depleted.

The pattern exposure was carried out for the sample with the BP concentrations of  $9 \text{ wt. \%}$ ,  $19 \text{ wt. \%}$ , and  $41 \text{ wt. \%}$  vs PMMA, and the exposure doses were as high as  $40.6 \text{ J/cm}^2$  at  $365 \text{ nm}$  of broad light exposure. Atomic hydrogen dry development patterning was successfully carried out for all three BP concentrations (Fig. 3 and Fig. S2 in the supplementary material). Figure 3 shows the results for the sample of PMMA with  $19 \text{ wt. \% BP}$  obtained with broad light exposure and  $9 \text{ min}$  of atomic hydrogen dry development. The etched area was the masked area composed of PMMA and BP. This reaction system acted as a negative tone resist. For the  $19 \text{ wt. \% BP}$  samples, the exposure doses of  $2.2 \text{ J/cm}^2$ ,  $6.5 \text{ J/cm}^2$ ,  $13.8 \text{ J/cm}^2$ , and  $29.1 \text{ J/cm}^2$  were also tested for pattern exposure in addition to the  $40.6 \text{ J/cm}^2$  exposure, and all of the samples were successfully dry-developed by atomic hydrogen etching, as shown in Fig. S3 in the supplementary material.

The profiles of the remaining pattern of the  $19 \text{ wt. \% BP}$  sample treated with an exposure dose of  $40.6 \text{ J/cm}^2$  after the development are shown in Fig. 4. As observed from the figure, the etched patterns were trapezoidal. For this sample, the duty ratio of the exposed and unexposed areas was  $1.15:1$  for both the positive and negative patterns, and the original mask pattern had a ratio of  $1:1$ . This widening of the exposed area can be understood as being due to the reflection of light between the photo-mask and the Si substrate in the polymer layer in addition to the diffraction of light at the photo-mask.

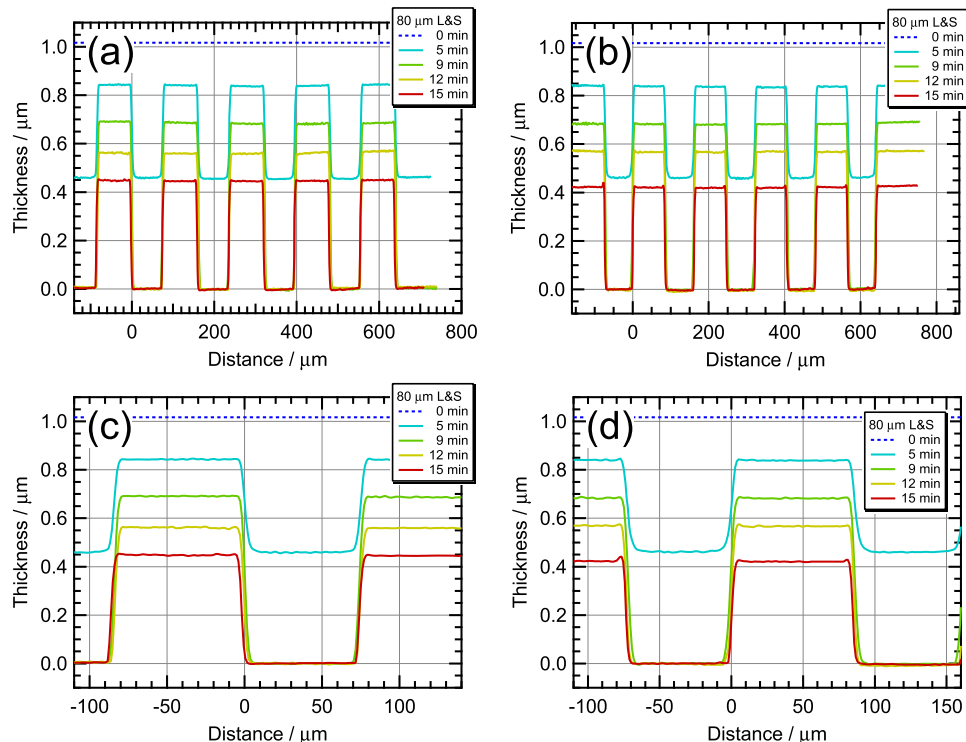


**FIG. 4.** Remaining film profiles after atomic hydrogen dry development for the films of PMMA with  $19 \text{ wt. \% BP}$  with broad light exposure of  $40.6 \text{ J/cm}^2$  at  $365 \text{ nm}$ . The presented patterns correspond to the  $80 \mu\text{m}$  line and space mask pattern. Positive pattern area (a) and negative pattern area (b) and their expanded plots [(c) and (d)] are shown. Zero height corresponds to the silicon substrate surface. For the  $5 \text{ min}$  development plots, the remaining layer thicknesses were determined from the Si substrate and were used as offsets.

These unwanted exposure effects under the photo-mask limit clean patterning. When the exposure dose decreased to  $2.2 \text{ J/cm}^2$ , the ratio decreased to 1.07:1 under the same development conditions (Fig. S4). Therefore, unwanted exposure contributed mainly to the duty ratio. As expected from the dependence of the selection ratio on the concentration, there was no duty ratio dependence on the concentration for the samples with BP concentrations of 9 wt. %, 19 wt. %, and 41 wt. %. The sidewall angles obtained for the samples with 9 min, 12 min, and 15 min development shown in Fig. 4 were  $7.6^\circ$ ,  $7.2^\circ$ , and  $6.4^\circ$ , respectively. These values are far from the values of the conventional resist (close to  $90^\circ$ ) and are reasonable for the hard contact exposure of broad light that causes the unwanted exposure mentioned above. In addition, the selection ratio was small, and the isotropic nature of the dry etching technique led to the sloping of the edges. While it would be interesting to estimate the critical dimension and the ultimate resolution of the present technique, it is better to omit the estimation of these values to avoid an incorrect estimation of the characteristics of the dry development using atomic hydrogen because the present results are too far from those of the best available exposure techniques. Furthermore, the resists used in the present experiments are obtained for a model reaction system composed of BP and PMMA, and  $1 \mu\text{m}$  line and space patterning, as shown in Fig. S5 in the [supplementary material](#). Thus, the results obtained for this system may not be suitable for estimating the critical dimension and the ultimate resolution of this technique, but at least less than  $1 \mu\text{m}$  resolution will be possible. To obtain more refined patterns, it will be necessary to access reduced projection exposure using an anti-reflection coating. Because the goal of this experiment is to report and demonstrate a proof-of-concept system for a new dry development approach, a detailed characterization of the obtained pattern is beyond the scope of this paper.

## CONCLUSIONS

The application of atomic hydrogen was expanded to photolithography. A novel photolithographic process using atomic hydrogen dry development was proposed and successfully demonstrated. A PMMA thin film containing benzophenone was used as a model reaction system, and pattern exposure was carried out with broad light irradiation. The dependence of the selection ratio on the exposure dose was determined, and a maximum selection ratio of 3.2 was achieved for 41 wt. % BP-containing PMMA with an exposure dose of  $40.6 \text{ J/cm}^2$  at 365 nm. Photolithographic patterning was successfully performed using the exposure doses of  $2.2 \text{ J/cm}^2$ ,  $4.7 \text{ J/cm}^2$ ,  $13.5 \text{ J/cm}^2$ ,  $29.1 \text{ J/cm}^2$ , and  $40.6 \text{ J/cm}^2$  at 365 nm.

The proposed procedure can be summarized as follows. A thin film, composed of a polymer that can be easily etched by atomic hydrogen irradiation and a photosensitizer, was fabricated. The photosensitizer must be sublimable under reduced pressure at the temperature of the dry-etching condition and able to undergo a photo-reaction with the base polymer. The polymer produced by the photochemical reaction changed the etching rate of atomic hydrogen dry etching. Then, a pattern exposure of light that can cause photo-reaction of the photosensitizer was applied. Finally, the sample was irradiated with atomic hydrogen to carry out dry development.

## SUPPLEMENTARY MATERIAL

See the supplementary material for exposure dose and BP concentration dependences on the selection ratio (log-log plot) (Fig. S1), optical microscopy images of atomic hydrogen dry development photolithography (9 and 41 wt. % BP) (Fig. S2), optical microscopy images of photolithography (exposure dose dependence) (Fig. S3), remaining film profiles after atomic hydrogen dry development on 19 wt. % BP vs PMMA film and their differential values of thickness by distance (Fig. S4), and optical microscopy images of photolithography of less than  $6 \mu\text{m}$  lines and spaces (Fig. S5).

## ACKNOWLEDGMENTS

The authors would like to thank Mr. Koki Tamura and Mr. Satoshi Oya of Tokyo Ohka Kogyo Co., Ltd., for their help in our experiments.

## DATA AVAILABILITY

The data that support the findings of this study are available from the corresponding author upon reasonable request.

## REFERENCES

- H. Horibe, M. Yamamoto, E. Kusano, T. Ichikawa, and S. Tagawa, *J. Photopolym. Sci. Technol.* **21**, 293 (2008).
- M. Yamamoto, H. Horibe, H. Umemoto, K. Takao, E. Kusano, M. Kase, and S. Tagawa, *Jpn. J. Appl. Phys., Part 1* **48**, 026503 (2009).
- M. Yamamoto, T. Maruoka, A. Kono, H. Horibe, and H. Umemoto, *Jpn. J. Appl. Phys., Part 1* **49**, 016701 (2010).
- A. Kono, Y. Arai, Y. Goto, M. Yamamoto, S. Takahashi, T. Yamagishi, K. Ishikawa, M. Hori, and H. Horibe, *Thin Solid Films* **575**, 17 (2015).
- S. Takagi, T. Nishiyama, M. Yamamoto, E. Sato, T. Kamimura, T. Ogata, and H. Horibe, *J. Photopolym. Sci. Technol.* **29**, 629 (2016).
- A. Matsuo, S. Takagi, T. Nishiyama, M. Yamamoto, E. Sato, and H. Horibe, *J. Photopolym. Sci. Technol.* **31**, 369 (2018).
- H. N. Wanka and M. B. Schubert, *J. Phys. D: Appl. Phys.* **30**, L28 (1997).
- A. Izumi, H. Sato, S. Hashioka, M. Kudo, and H. Matsumura, *Microelectron. Eng.* **51-52**, 495 (2000).
- V. Ramachandran, M. F. Brady, A. R. Smith, R. M. Feenstra, and D. W. Greve, *J. Electron. Mater.* **27**, 308 (1998).
- H. Ohmi, J. Sato, T. Hirano, Y. Kubota, H. Kakiuchi, and K. Yasutake, *Appl. Phys. Lett.* **109**, 211603 (2016).
- I. Langmuir, *J. Am. Chem. Soc.* **34**, 860 (1912).
- R. W. Wood, *London, Edinburgh, Dublin Philos. Mag. J. Sci.* **44**, 538 (1922).
- H. Matsumura, H. Umemoto, K. K. Gleason, and R. E. I. Schropp, *Catalytic Chemical Vapor Deposition* (Wiley, 2019).
- E. Ekinci, in *Hydrogen Energy System* (Springer Netherlands, 1995), pp. 111–133.
- C. Yan, H. Mao, W. Li, J. Qian, Y. Zhao, and R. J. Hemley, *Phys. Status Solidi* **201**, R25 (2004).
- G. Shivkumar, S. S. Tholeti, M. A. Alrefae, T. S. Fisher, and A. A. Alexeenko, *J. Appl. Phys.* **119**, 113301 (2016).
- G. E. Moore and F. C. Unterwald, *J. Chem. Phys.* **40**, 2639 (1964).
- F. Jansen, I. Chen, and M. A. MacHonkin, *J. Appl. Phys.* **66**, 5749 (1989).
- Y. Goto, Y. Angata, E. Tsukazaki, S. Takahashi, K. Koike, T. Yamagishi, and H. Horibe, *Jpn. J. Appl. Phys., Part 1* **53**, 02BB04 (2014).
- Y. Goto, K. Kitano, T. Maruoka, M. Yamamoto, A. Konno, H. Horibe, and S. Tagawa, *J. Photopolym. Sci. Technol.* **23**, 417 (2010).
- Z. Czech, *Polym. Bull.* **52**, 283 (2004).

- <sup>22</sup>F. Rahman, D. J. Carbaugh, J. T. Wright, P. Rajan, S. G. Pandya, and S. Kaya, *Microelectron. Eng.* **224**, 111238 (2020).
- <sup>23</sup>A. Salmassi and W. Schnabel, *Polym. Photochem.* **5**, 215 (1984).
- <sup>24</sup>C. Walling and M. J. Gibian, *J. Am. Chem. Soc.* **87**, 3361 (1965).
- <sup>25</sup>G. Morales, E. Castro, E. Kaluyzhnaya, and R. Guerrero-Santos, *J. Appl. Polym. Sci.* **57**, 997 (1995).
- <sup>26</sup>Y. Ito, Y. Aoki, T. Matsuura, N. Kawatsuki, and M. Uetsuki, *J. Appl. Polym. Sci.* **42**, 409 (1991).
- <sup>27</sup>D. M. Dankbar and G. Gauglitz, *Anal. Bioanal. Chem.* **386**, 1967 (2006).
- <sup>28</sup>T. Ohtake, T. Takaoka, and M. Nakagawa, *Kobunshi Ronbunshu* **66**, 111 (2009).
- <sup>29</sup>T. Ohtake, H. Oda, T. Takaoka, and M. Nakagawa, *J. Photopolym. Sci. Technol.* **22**, 205 (2009).